Published in final edited form as:
J Immunol. 2014 September 15; 193(6): 2881–2890. doi:10.4049/jimmunol.1302201.

The Ataxia Telangiectasia Mutated and Cyclin D3 Proteins Cooperate to Help Enforce TCRβ and IgH Allelic Exclusion

Natalie C. Steinel[*,†,‡], **Megan R. Fisher**[*,†,‡], **Katherine S. Yang-Iott**[*,†], and **Craig H. Bassing**[*,†,‡,§]

[*]Division of Cancer Pathobiology, Department of Pathology and Laboratory Medicine, Center for Childhood Cancer Research, Children's Hospital of Philadelphia, Philadelphia, PA

[†]Abramson Family Cancer Research Institute, Department of Pathology and Laboratory Medicine, Perelman School of Medicine at the University of Pennsylvania, Philadelphia, PA

[‡]Immunology Graduate Group, Perelman School of Medicine at the University of Pennsylvania, Philadelphia, PA

Abstract

Coordination of V rearrangements between loci on homologous chromosomes is critical for Ig and TCR allelic exclusion. The Ataxia Telangietasia mutated (ATM) protein kinase promotes DNA repair and activates checkpoints to suppress aberrant Ig and TCR rearrangements. In response to RAG cleavage of Igκ loci, ATM inhibits RAG expression and suppresses further Vκ-to-Jκ rearrangements to enforce Igκ allelic exclusion. Since V recombination between alleles is more strictly regulated for TCRβ and IgH loci, we evaluated the ability of ATM to restrict bi-allelic expression and V-to-DJ recombination of TCRβ and IgH genes. We detected greater frequencies of lymphocytes with bi-allelic expression or aberrant V-to-DJ rearrangement of TCRβ or IgH loci in mice lacking ATM. A pre-assembled DJβ complex that decreases the number of TCRβ rearrangements needed for a productive TCRβ gene further increased frequencies of ATM-deficient cells with bi-allelic TCRβ expression. IgH and TCRβ proteins drive proliferation of pro-lymphocytes through Cyclin D3, which also inhibits V_H transcription. We show that inactivation of Cyclin D3 leads to increased frequencies of lymphocytes with bi-allelic expression of IgH or TCRβ genes. We also show that Cyclin D3 inactivation cooperates with ATM deficiency to increase the frequencies of cells with bi-allelic TCRβ or IgH expression, while decreasing the frequency of ATM-deficient lymphocytes with aberrant V-to-DJ recombination. Our data demonstrate that core components of the DNA damage response and cell cycle machinery cooperate to help enforce IgH and TCRβ allelic exclusion, and indicate that control of V-to-DJ rearrangements between alleles is important to maintain genomic stability.

[§]Corresponding author: Craig H. Bassing, Ph.D., 4054 Colket Translational Research Building, 3501 Civic Center Boulevard, Philadelphia, PA 19104, bassing@email.chop.edu, Phone: 267-426-0311, FAX: 267-426-2791.
[1]M.C.S. and M.R.F. contributed equally to this work.

[3]None of the authors have any conflicts of interest.

NIH-PA Author Manuscript
NIH-PA Author Manuscript

Introduction

Antigen receptor diversity is generated through assembly of T cell antigen receptor (TCR) and immunoglobulin (Ig) genes from variable (V), diversity (D), and joining (J) gene segments. The RAG1 and RAG2 proteins introduce DNA double strand breaks (DSBs) adjacent to gene segments, forming hairpin-sealed coding ends and blunt signal ends (1). RAG proteins cooperate with ATM to hold these chromosomal DNA ends in post-cleavage complexes and facilitate their repair by non-homologous end-joining (NHEJ) factors, which form coding and signal joins (2). V(D)J coding joins form the second exons of Ig and TCR genes, which are transcribed with constant (C) region exons. The combination of joining events, imprecise processing of coding ends, and pairing of different Ig or TCR proteins cooperate to create antigen receptor diversity.

Complete assembly of most Ig and TCR genes occurs only on one allele at a time, indicating the importance of mechanisms that control recombination between alleles (3-5). Ability of Ig and TCR chains expressed from one allele to signal feedback inhibition of V rearrangements on the other allele ensures their mono-allelic expression (allelic exclusion) on most lymphocytes (3-5). Asynchronous initiation of V rearrangements between loci on homologous chromosomes is likely required for feedback inhibition to enforce allelic exclusion (3-5). In addition, ability of V(D)J recombination events on one allele to activate signals that transiently suppress V rearrangements on the other allele has been hypothesized to be important for feedback inhibition to mediate allelic exclusion (6). Consistent with this notion, we recently showed that RAG DSBs induced during Igκ recombination on one allele signal through ATM to down-regulate RAG expression, inhibit further Vκ-to-Jκ rearrangements on the other allele, and enforce Igκ allelic exclusion (7,8).

Assembly and expression of TCRβ and IgH genes is more stringently controlled than Igκ genes. TCRβ and IgH genes assemble through D-to-J recombination, and then rearrangement of V segments to assembled DJ complexes on one allele at a time (9,10). TCRβ and IgH D-to-J recombination are not controlled by feedback inhibition, while Vβ and V_H rearrangements are controlled by feedback inhibition (9,10). In one-third of pro-lymphocytes, assembly and expression of in-frame TCRβ or IgH genes on the first allele generates pre-receptor complexes that signal feedback inhibition of V-to-DJ rearrangements on the other allele (9,10). These pre-receptors also signal activation of Cyclin D3 (Ccnd3) protein expression to drive proliferation as cells differentiate into pre-lymphocytes (11-13). The two-thirds of pro-lymphocytes that assemble out-of-frame TCRβ or IgH genes can initiate V-to-DJ rearrangements on the other allele in a second attempt to assemble an in-frame VDJ rearrangement required for differentiation. As a result, ~60% of cells assembles VDJ rearrangements on one allele, and ~40% assembles VDJ rearrangements on both alleles, with one of these out-of-frame in most cells (9,10). This limits bi-allelic surface expression of TCRβ chains to ~1% of mature αβ T cells and of IgH chains to ~0.01% of mature B cells (14-17). In pre-B cells, Igκ genes assemble through Vκ-to-Jκ recombination on one allele at a time (18-20). Assembly of functional Igκ genes in pre-B cells can generate innocuous BCRs that suppress additional Vκ-to-Jκ rearrangements and promote differentiation (19,20). However, most BCRs are autoreactive and induce further Igκ rearrangements, which occur on either allele (19-21). Therefore, ~10% of pre-B cells assembles in-frame VκJκ rearrangements on both alleles (21). Yet, this results in equal high-level expression of Igκ chains from both alleles on only ~3% of B cells due to inability of one Igκ chain to pair with the available IgH chain in many cells (21,22).

Considering distinct features and differential regulation of V rearrangements between Igκ loci and IgH/TCRβ loci, it is important to determine the ability of ATM to coordinate V-to-DJ recombination between alleles and enforce allelic exclusion of IgH and TCRβ genes. We previously demonstrated that *Atm*$^{-/-}$ pro-B cells exhibit an increased frequency of γ-H2AX foci (a marker for DSBs) on both alleles (7). These data could result from loss of ATM signals that control initiation of IgH recombination between alleles or impaired DSB repair leading to V(D)J recombination on the second allele before transduction of IgH feedback signals from the first allele. Although we did not observe a profound violation of IgH allelic exclusion on mature B cells of *Atm*$^{-/-}$ mice (7), we neither determined whether the increased frequency of B cells expressing IgH chains from both alleles was significant nor considered the impact of aberrant IgH recombination on bi-allelic IgH expression. Here, we monitor allele-specific TCRβ and IgH expression on and visualize TCRβ and IgH rearrangements in mature lymphocytes from *Atm*$^{-/-}$ and wild-type mice. We show that ATM helps enforce TCRβ and IgH allelic exclusion by inhibiting bi-allelic V-to-DJ recombination. We demonstrate that Cyclin D3 also helps enforce TCRβ and IgH allelic exclusion alone and in cooperation with ATM. Finally, we show that decreasing aberrant Vβ or V_H rearrangements in *Atm*$^{-/-}$ cells further increases the frequencies of lymphocytes with bi-allelic TCRβ or IgH expression. Our data demonstrate that core components of the DNA damage response and cell cycle machinery cooperate to help enforce IgH and TCRβ allelic exclusion, and indicate that coordination of V-to-DJ recombination between alleles is important to maintain genomic stability.

Materials and Methods

Mice

All mice were on a 129/C57B6 mixed background, and bred and housed under specific pathogen-free conditions at the Children's Hospital of Philadelphia (CHOP). None of the *Atm*$^{-/-}$ mice analyzed in this study showed evidence of a subclinical but emerging thymic lymphoma, as assayed Southern blotting or PCR for oligoclonal TCRβ rearrangements or by flow cytometry for increased number/frequency of TCRβ^{-} CD4^{+}CD8^{+} or TCRβ^{-} CD8^{+} thymocytes. All animal husbandry and experiments were performed in accordance with national guidelines and regulations and were approved by the CHOP Institutional Animal Care and Use Committee.

Preparation of single cell suspension for flow cytometry

Single cell suspensions for flow cytometry were isolated from the thymus, bone marrow, and spleens of six-week-old mice. Cells were harvested and stained in PBS containing 3% FCS and 0.25mM EDTA. Prior to staining, suspensions were depleted of red blood cells with NH_4Cl lysis buffer and FC receptors were blocked using anti-CD16/CD32 (2.4G2, BD Pharmingen). Data were collected on an LSR II and analyzed with FlowJo. Single, live cells were gated on the basis of forward and side scatter and DAPI exclusion (Invitrogen).

Flow cytometric analysis of Vβ surface expression

Stains were conducted using the following antibodies or reagents from BD Bioscience: APC/Cy7-anti-mouse B220 (RA3-6B2), APC-anti-mouse TCRβ (H57-597), FITC-anti-mouse Vβ5 (MR9-4), FITC-anti-mouse Vβ14 (14-2), PE-anti-mouse Vβ8 (F23.1), PE-anti-mouse Vβ10b (B21.5), biotin-anti-mouse Vβ4 (KT4), biotin-anti-mouse Vβ6 (RR4-7), biotin-anti-mouse Vβ12 (MR11-1) and PE/Cy7-streptavidin. Surface Vβ expression was assayed on single, $DAPI^{-}$, $B220^{-}$, $TCR\beta^{+}$ cells.

Flow cytometric analysis of IgM surface expression

Stains were conducted using the following antibodies or reagents: FITC-anti-mouse IgMα (DS-1, BD Bioscience), PE-anti-mouse IgMβ (AF6-78, BD Bioscience), Biotin-anti-mouse CD23 (B3B4, BD Bioscience), PerCP/Cy5.5-anti-mouse CD21/35 (7E9, BioLegend), PE/Cy7-SA (BD Bioscience). Surface IgM expression was assayed on single, $DAPI^{-}$, $TCR\beta^{-}$, $B220^{+}$ cells.

Stimulation of αβ T cells for generation of hybridomas and for 2C-FISH assays

Single cell suspensions were isolated from the spleens of six-week-old mice and depleted of red blood cells with NH_4Cl lysis buffer prior to stimulation. Each spleen was stimulated for 48 hours in 40 units/ml IL-2 and 5 μg/ml ConA, at 4ml/spleen in DMEM containing 15% FBS, 1% Penicillin/Streptomycin, 1% L-gluatmate and 30μM β-Mercaptoethanol. Additional media was added to the stimulation after 24 hours.

Fusion and analysis of αβ T cell hybridomas

Hybridomas were produced by fusion of ConA/IL-2 stimulated splenic αβ T cells with BW-1100.129.237 thymoma cells. Southern analysis of TCRβ rearrangements was performed as previously described (23,24)

Stimulation of splenic B cells for 2C-FISH

Single cell suspensions isolated from the spleens of six-week-old mice were depleted of red blood cells with NH_4Cl lysis buffer prior to stimulation. Spleen cells were stimulated for 48 hours in 1μM CpG ODN1826 at 0.5×10^6 cell/ml in RPMI containing 10% FBS, 1% Penicillin/Streptomycin, 1% L-glutamate, 1% NEAA, 30μM β-mercaptoethanol, 1% HEPES, and 1% OPI.

2C-FISH assays

B and T cells stimulated for 48 hours were arrested in metaphase by incubating with 0.0μg/mL colcemid (KaryoMax) and 0.45mM BrdU (Sigma) for 2 hours. Metaphase arrested cells were isolated by hypotonic treatment (40mM KCl, 0.5mM EDTA, 20mM HEPES, pH7.4) and fixation in methanol:acetic acid (3:1 volume). The fixed cells were then dropped on slides at 4°C and dried at 75°C for 5 minutes. Metaphase spreads were hybridized overnight with relevant *Tcrb* and *Igh* bacterial artificial chromosome (BAC) probes: Vβ-DβJβ1, RP23-203H5; Cβ, 164G11; V_H-D_H, RP24-275L15, and 3'IgH, CT7-199M11. Cβ and 3'IgH probes were labeled using the DIG-NICK Translation Mix (Roche). Vβ-DβJβ1 and V_H-D_H probes were labeled using the BioPrime DNA Labeling

System (Invitrogen). Probes were detected using Fitc-anti-digoxin Fab (Roche) and Texas red-streptavidin (Vector Laboratories). Coverslips were mounted with Vectasheild mounting medium with DAPI (Vector). Images were captured and analyzed using Case Data Manager (Applied Spectral Imaging).

Statistical Analyses

All p values were generated by two-tailed Student's *t* test using Prism (GraphPad Software).

Results

ATM inhibits bi-allelic expression and recombination of Vβ segments and suppresses aberrant Vβ-to-DJβ rearrangements

To determine the effect of ATM on TCRβ allelic exclusion, we used flow cytometry to quantify the percentages of αβ T cells from $Atm^{-/-}$ or wild-type (*WT*) mice that express cell surface TCRβ chains from both alleles. Since an allotypic marker has not been found or generated for mouse TCRβ chains, only anti-Vβ antibodies can identify expression of TCRβ chains from both alleles on mouse αβ T cells. However, due to the absence of anti-Vβ antibodies for all mouse Vβ peptides, this underestimates the actual frequency of bi-allelic TCRβ expression. We used 14 distinct combinations of available anti-Vβ antibodies to monitor TCRβ expression from both alleles on αβ T cells isolated from the thymuses or spleens of age-matched littermate $Atm^{-/-}$ or *WT* mice. We conducted this cellular analysis on $TCR\beta^{high}$ thymocytes and on $TCR\beta^{+}$ splenocytes. As compared to *WT* mice, we detected significantly higher percentages of $V\beta14^{+}V\beta8^{+}$ (p=0.0019) and $V\beta14^{+}V\beta6^{+}$ (p=0.0197) thymic αβ T cells and of $V\beta8^{+}V\beta12^{+}$ (p=0.0497) and $V\beta8^{+}V\beta6^{+}$ (p=0.0077) splenic αβ T cells from $Atm^{-/-}$ mice (Fig. 1*A*,*B*). The frequencies of these αβ T cells that express TCRβ chains from both alleles were 1.3 to 1.6 fold higher in $Atm^{-/-}$ mice relative to *WT* mice (Fig. 1*B*). We also observed higher frequencies of αβ T cells expressing two different Vβ peptides for most other combinations of anti-Vβ antibodies, although none of these differences reached significance with the numbers of mice analyzed (Fig. 1*B*). These data suggest that ATM helps enforce TCRβ allelic exclusion.

In addition to asynchronous initiation and feedback inhibition of Vβ-to-DJβ rearrangements, post-transcriptional silencing of in-frame TCRβ genes controls TCRβ allelic exclusion (25). Therefore, to determine whether ATM helps enforce TCRβ allelic exclusion by limiting the frequency of mature αβ T cells with bi-allelic Vβ-to-DβJβ recombination, we analyzed TCRβ rearrangements in a panel of αβ T cell hybridomas that we made from $Atm^{-/-}$ mice. The TCRβ locus consists of 34 upstream Vβ segments, two Dβ-Jβ-Cβ clusters, and the downstream Vβ14 segment (Fig. 1*C*). All TCRβ rearrangements delete intervening sequences, except for Vβ14-to-DβJβ rearrangements that occur through inversion. To analyze TCRβ rearrangements, we conducted Southerns on *EcoR*I-digested hybridoma DNA using 3’Jβ2, 3’Jβ1, and 5’Dβ1 probes (Fig. 1*C*). Hybridization of 3’Jβ2 and 3’Jβ1 probes to non-germline fragments identifies alleles with DβJβ and/or VβDβJβ rearrangements. Hybridization of the 5’Dβ1 probe to non-germline fragments identifies alleles with DβJβ or Vβ14DβJβ rearrangements, while lack of 5’Dβ1 probe hybridization reveals alleles with VβDβJβ rearrangements involving upstream Vβs. By this approach, we identified 76 hybridomas with VβDβJβ rearrangements on both alleles, and 70 hybridomas with VβDβJβ rearrangements on one allele and DβJβ rearrangements on the other allele (Fig. 1*D*). At first approximation, these data suggest that 48% of *Atm*$^{-/-}$ αβ T cells contains VβDβJβ rearrangements on one allele and 52% contains VβDβJβ rearrangements on both alleles, consistent with a role for ATM in coordinating Vβ recombination between alleles. However, we also identified 44 hybridomas with VβDβJβ rearrangements on one allele, but no 3'Jβ2, 3'Jβ1, or 5'Dβ1 probe hybridization on the other allele, indicative of aberrant TCRβ rearrangements on non-selected alleles in these cells (Fig. 1*D*). Since ATM prevents RAG DSBs from aberrantly resolving as small chromosomal deletions (26), both Dβ-to-Jβ and Vβ-to-DβJβ recombination in *Atm*$^{-/-}$ cells could lead to loss of sequences to which the 3'Jβ2, 3'Jβ1, and 5'Dβ1 probes hybridize. Accordingly, our Southern analysis of TCRβ rearrangements in *Atm*$^{-/-}$ αβ T cell hybridomas prevents any conclusion regarding whether ATM suppresses the frequency of mature αβ T cells with bi-allelic Vβ rearrangements.

To determine whether ATM inhibits bi-allelic Vβ rearrangements, we needed approaches to isolate the Vβ-to-DβJβ recombination step and capture aberrant Vβ rearrangements that delete 3'DJβ sequences. We previously created and characterized *Jb1*$^{DJ/DJ}$ mice with TCRβ alleles that contain a pre-assembled DβJβ1 complex, lack the Dβ2-Jβ2 cluster, and are only capable of Vβ recombination (24). Because αβ T cells from *Jb1*$^{DJ/DJ}$ mice exhibit normal frequencies of bi-allelic TCRβ expression and VβDβJβ rearrangements (24), we generated and analyzed *Atm*$^{-/-}$*Jb1*$^{DJ/DJ}$ mice to isolate the Vβ-to-DβJβ recombination step. We used the same 14 combinations of available anti-Vβ antibodies to monitor TCRβ expression from both alleles on TCRβ^{high} thymocytes or TCRβ^{+} splenocytes isolated from age-matched littermate *Atm*$^{-/-}$*Jb1*$^{DJ/DJ}$ or *Atm*$^{+/+}$*Jb1*$^{DJ/DJ}$ mice. As compared to *Atm*$^{+/+}$*Jb1*$^{DJ/DJ}$ mice, we detected 1.6 to 2.6 fold higher percentages of Vβ14^{+}Vβ8^{+} (p=0.0008), Vβ8^{+}Vβ12^{+} (p=0.0007), Vβ14^{+}Vβ6^{+} (p=0.0067), and Vβ5^{+}Vβ6^{+} (p=0.004) thymic αβ T cells and of Vβ14^{+}Vβ6^{+} (p=0.0001), Vβ5^{+}Vβ12^{+} (p=0.0133), and Vβ5^{+}Vβ6^{+} (p=0.0016) splenic αβ T cells from *Atm*$^{-/-}$*Jb1*$^{DJ/DJ}$ mice (Fig. 2*A,B*). We also observed higher frequencies of cells expressing two different Vβ peptides for most other combinations of anti-Vβ antibodies, with many of these differences significant (Fig. 2*B*). These data indicate that preventing aberrant Dβ-to-Jβ recombination increases the frequency of mature *Atm*$^{-/-}$ αβ T cells that express TCRβ chains from both alleles.

To capture aberrant Vβ-to-DβJβ rearrangements that lead to deletion of 3'DβJβ sequences, we developed a two-color fluorescence *in situ* hybridization (2C-FISH) approach to quantify Vβ-to-DβJβ recombination in age-matched littermate *Atm*$^{-/-}$*Jb1*$^{DJ/DJ}$ and *Atm*$^{+/+}$*Jb1*$^{DJ/DJ}$ αβ T cells. We conducted 2C-FISH on metaphases prepared from *ex vivo* stimulated splenic αβ T cells using probes that hybridize to sequences between the upstream Vβ segments and Dβ1 (Vβ-Dβ1 probe) or downstream of the pre-assembled DβJβ1 complex (Cβ probe)(Fig. 2*C*). Co-hybridization of both probes identifies alleles with no VβDβJβ rearrangements, or those involving Vβ14 that occur in ~5% of αβ T cells (23). Hybridization of only the Cβ probe identifies alleles with VβDβJβ rearrangements. The Cβ probe can hybridize to alleles with deletion of 3'DβJβ1 sequences to which the 3'Jβ1 and 3'Jβ2 Southern probes cannot hybridize, and therefore scores aberrant Vβ-to-DβJβ rearrangements that could not be captured in our Southern analysis of hybridomas. Hybridization of both probes on different chromosomes identifies TCRβ translocations that also could not be captured in our hybridoma analysis. We detected a probe hybridization pattern indicative of VβDβJβ rearrangements on both alleles in a significantly greater percentage of $Atm^{-/-}Jb1^{DJ/DJ}$ cells as compared to $Atm^{+/+}Jb1^{DJ/DJ}$ cells (45.0% +/−3.6% vs 35.3% +/−2.1%, p=0.0372)(Fig. 2*D*,*E*). Consistent with this observation, we also detected a probe hybridization pattern indicative of VβDβJβ rearrangement on only one allele in a smaller fraction of $Atm^{-/-}Jb1^{DJ/DJ}$ cells relative to $Atm^{+/+}Jb1^{DJ/DJ}$ cells (52.2% +/− 2.7% vs 64.5% +/− 2.0%, p=0.013)(Fig. 2*D*,*E*). These frequencies of VβDβJβ rearrangements are underestimates because our assay cannot capture the ~5% of alleles containing Vβ14-to-DβJβ recombination (27). We also observed probe hybridization patterns indicative of a normal VβDβJβ rearrangement on one allele and an aberrant VβDβJβ rearrangement (mostly Cβ deletions) on the other allele in a greater percentage of $Atm^{-/-}Jb1^{DJ/DJ}$ cells as compared to $Atm^{+/+}Jb1^{DJ/DJ}$ cells (2.8% +/− 1.4% vs 0.2% +/− 0.2%, p=0.0442)(Fig. 2*D-F*). Therefore, our 2C-FISH analysis of TCRβ rearrangements in $Atm^{-/-}Jb1^{DJ/DJ}$ and $Atm^{+/+}Jb1^{DJ/DJ}$ αβ T cells demonstrate that ATM helps enforce TCRβ expression allelic exclusion by suppressing the frequency of cells with Vβ-to-DβJβ recombination on both alleles.

ATM limits bi-allelic IgH expression and suppresses aberrant IgH rearrangements

To determine whether ATM limits bi-allelic IgH expression, we used $Igh^{a/b}$ mice that contain an allotypic marker that enables analysis of surface IgM expression from each allele using anti-IgM^a and anti-IgM^b antibodies (16). Although this approach provides a more accurate measurement of bi-allelic IgH expression than anti-Vβ flow cytometry for TCRβ chains, it cannot detect IgH chain expression on Ig class switched cells and therefore also underestimates the frequency of bi-allelic IgH expression. Since ~1/3 of $V_HD_HJ_H$ rearrangements assemble in-frame and IgH chains are required for differentiation, 20% is the maximal frequency of B cells that can exhibit IgH allelic inclusion assuming V_H rearrangements on both alleles, no IgH feedback inhibition, and no selection for/against dual-IgM^+ cells (28). Yet, due to asynchronous initiation and IgH-mediated feedback inhibition of V_H recombination, impaired coding join formation in $Atm^{-/-}$ cells (29) and IgH/Igκ chain pairing restrictions (30), significantly less than 20% of $Atm^{-/-}Igh^{a/b}$ cells would express surface IgM chains from both alleles if ATM controls V_H recombination between alleles. Although ~7% of splenic mouse B cells expresses Igκ chains from both alleles, only ~3% expresses equivalent high levels of Igκ chains from both alleles as determined by an appropriate gate (21). We used a similar gating strategy to demarcate mature B cells expressing equivalent high levels of IgH chains from both alleles. In each experimental replicate, we determined the position of this gate from a 1:1 mix of $Igh^{a/a}$ and $Igh^{b/b}$ stained cells so as to include any cells that express IgH from a single allele (Fig. 3*A*). Using this approach, we observed equivalent high-level expression of IgM^a and IgM^b on ~1.6-fold greater percentages of total $B220^+$ bone marrow and splenic B cells from $Atm^{-/-}Igh^{a/b}$ mice as compared to age-matched littermate $Igh^{a/b}$ mice (bone marrow: 0.41 +/− 0.06% vs 0.24 +/−0.04%, p=0.045; spleen: 0.98 +/− 0.07% vs 0.65 +/− 0.05%, p=0.002) (Fig. 3*A*,*B*). These data demonstrate that ATM helps enforce IgH expression.

To determine whether ATM helps enforce IgH allelic exclusion by inhibiting the frequency of mature B cells with bi-allelic V_H rearrangements, we used 2C-FISH with V_H-D_H and

3'IgH probes (Fig. 3*C*) to quantify V_H-to-D_HJ_H recombination in splenic B cells of age-matched littermate *Atm*$^{-/-}$ and *WT* mice. We detected probe hybridization pattern indicative of a $V_HD_HJ_H$ rearrangement on one allele and a D_HJ_H rearrangement on the other allele in a smaller fraction of *Atm*$^{-/-}$ cells relative to *WT* cells (43.3% +/− 2.4% vs 60.8% +/−4.4 %, p=0.0125)(Fig. 3*D*,*E*). We observed probe hybridization pattern indicative of bi-alelic $V_HD_HJ_H$ rearrangements in similar percentage of *Atm*$^{-/-}$ cells as compared to *WT* cells (39.5% +/− 3.4% vs 37.3% +/− 4.3%, p=0.6923)(Fig. 3*D*,*E*). In addition, we observed probe hybridization pattern indicative of a normal $V_HD_HJ_H$ rearrangement on one allele and an aberrant IgH rearrangement (mostly C_H deletions) on the other allele in a greater percentage of *Atm*$^{-/-}$ cells as compared to *WT* cells (17.2% +/− 2.2% vs 1.9% +/− 0.5%, p=0.0005) (Fig. 3*D-F*). These data are consistent with the notion that ATM helps enforce IgH allelic exclusion by limiting the frequency of mature B cells with V_H-to-D_HJ_H rearrangements on both alleles. However, since D_H-to-J_H, V_H-to-D_HJ_H, and class switch recombination can cause aberrant IgH rearrangements detected by FISH, and since mice with IgH alleles containing pre-assembled D_HJ_H complexes are unavailable, these data prevent conclusions about whether ATM suppresses the frequency of B cells with bi-allelic V_H-to-D_HJ_H recombination.

ATM cooperates with Cyclin D3 to limit bi-allelic IgH expression and V_H-to-D_HJ_H rearrangements

To determine whether ATM inhibits the frequency of B cells with bi-allelic V_H rearrangements, we sought to develop an approach to decrease the frequency of aberrant V(D)J recombination events that result in IgH translocations or C_H deletions. IgH expression in pro-B cells induces expression of Cyclin D3 (Ccnd3) to drive G1 progression and S phase entry (12). Since ATM suppresses aberrant V(D)J recombination in part by preventing cells with RAG DSBs from progressing into S phase (31,32), we reasoned that inactivation of Cyclin D3 would suppress translocations and C_H deletions in *Atm*$^{-/-}$ pro-B cells by enabling time to complete D_H-to-J_H and V_H-to-D_HJ_H rearrangements before S phase entry. Therefore, we created *Ccnd3*$^{-/-}$*Igh*$^{a/b}$ and *Ccnd3*$^{-/-}$*Atm*$^{-/-}$*Igh*$^{a/b}$ mice and analyzed IgH expression in splenic B cells of these and *Igh*$^{a/b}$ and *Atm*$^{-/-}$*Igh*$^{a/b}$ mice. We observed equivalent high-level expression of IgM^a and IgM^b on 1.34 +/− 0.04% of splenic B cells from *Ccnd3*$^{-/-}$*Igh*$^{a/b}$ mice and on 2.18 +/− 0.27% of splenic B cells from age-matched littermate *Ccnd3*$^{-/-}$*Atm*$^{-/-}$*Igh*$^{a/b}$ mice (Fig. 4*A*,*B*). The frequencies of B cells expressing high levels of surface IgM^a and IgM^b were ~1.6-fold greater in *Ccnd3*$^{-/-}$*Atm*$^{-/-}$*Igh*$^{a/b}$ mice relative to littermate *Ccnd3*$^{-/-}$*Igh*$^{a/b}$mice (p=0.0222) and ~2.2 fold greater as compared to age-matched *Atm*$^{-/-}$*Igh*$^{a/b}$ mice (p=0.005)(Fig. 4*B*). In addition, the frequency of splenic B cells expressing both IgM^a and IgM^b was ~2-fold higher in *Ccnd3*$^{-/-}$*Igh*$^{a/b}$ mice as compared to age-matched *Igh*$^{a/b}$ mice (p=0.0001) and ~3.3-fold higher in *Ccnd3*$^{-/-}$*Atm*$^{-/-}$*Igh*$^{a/b}$ mice relative to age-matched *Igh*$^{a/b}$ mice (p=0.0005) (Fig. 4*B*). Collectively, these data show that Cyclin D3 helps enforce IgH allelic exclusion alone and in cooperation with ATM.

To determine whether Cyclin D3 limits bi-allelic IgH expression by suppressing the frequency of B cells with V_H-to-D_HJ_H rearrangements on both alleles, we used 2C-FISH with V_H-D_H and 3'IgH probes to analyze IgH rearrangements in *Ccnd3*$^{-/-}$ and

Ccnd3$^{-/-}$*Atm*$^{-/-}$ splenic B cells. Our analysis of *Ccnd3*$^{-/-}$ metaphases scored a $V_HD_HJ_H$ rearrangement on one allele and a D_HJ_H rearrangement on the other allele in 54.1 +/− 1.2% of cells, normal $V_HD_HJ_H$ rearrangements on both alleles in 44.1 +/− 1.4% of cells, and a normal $V_HD_HJ_H$ rearrangement on one allele and C_H deletion on the other allele in 1.8 +/− 0.4% of cells (Fig. 4*C*). Although the frequency of bi-allelic $V_HD_HJ_H$ rearrangements was higher in *Ccnd3*$^{-/-}$ cells as compared to *WT* cells (Fig. 4*C*,*D*), this difference was not significant from the numbers of metaphases assayed. Our analysis of *Ccnd3*$^{-/-}$*Atm*$^{-/-}$ metaphases identified a $V_HD_HJ_H$ rearrangement on one allele and a D_HJ_H rearrangement on the other allele in 40.1 +/− 1.0% of cells, normal $V_HD_HJ_H$ rearrangements on both alleles in 51.5 +/− 1.5% of cells, and a normal $V_HD_HJ_H$ rearrangement on one allele and an aberrant IgH rearrangement (all being C_H deletions) on the other allele in 8.4 +/− 0.7% of cells (Fig. 4*C*-*E*). The frequency of metaphases with $V_HD_HJ_H$ rearrangements on both alleles was significantly higher in *Ccnd3*$^{-/-}$*Atm*$^{-/-}$ cells as compared to *Ccnd3*$^{-/-}$ (p=0.0184), *Atm*$^{-/-}$ (p=0.0396), and *WT* (p=0.0413) cells (Fig. 4*C*). This was associated with a significantly lower fraction of metaphases with a normal $V_HD_HJ_H$ rearrangement on one allele and an aberrant IgH rearrangement (all being C_H deletions) on the other allele in *Ccnd3*$^{-/-}$*Atm*$^{-/-}$ cells relative to *Atm*$^{-/-}$ cells (p=0.0215)(Fig. 4*C*-*E*). Notably, these data are consistent with published findings that half of the aberrant IgH rearrangements in *Atm*$^{-/-}$ splenic B cells arise from V(D)J recombination, while the remainder arise from class switch recombination (31). Since the frequencies of *Atm*$^{-/-}$ and *Atm*$^{-/-}$*Ccnd3*$^{-/-}$ splenic B cells with $V_HD_HJ_H$ rearrangements on one allele and D_HJ_H rearrangements on the other allele are equal, our data indicate that inactivation of Cyclin D3 increases bi-allelic IgH expression on *Atm*$^{-/-}$ B cells by suppressing the frequency of aberrant V_H-to-D_HJ_H rearrangements that delete C_H genes.

Cyclin D3 also cooperates with ATM to limit bi-allelic TCRβ expression

To determine whether Cyclin D3 also cooperates with ATM to limit bi-allelic TCRβ expression, we analyzed allele-specific TCRβ expression on splenic αβ T cells of *Ccnd3*$^{-/-}$ and *Ccnd3*$^{-/-}$*Atm*$^{-/-}$ mice. As compared to *Ccnd3*$^{-/-}$ mice, we detected 1.7 to 2.2 fold significantly higher percentages of Vβ14^{+}Vβ8^{+} (p=0.0236), Vβ8^{+}Vβ12^{+} (p=0.0238), Vβ14^{+}Vβ6^{+} (p=0.0118), Vβ5^{+}Vβ6^{+} (p=0.0344), Vβ14^{+}Vβ12^{+} (p=0.0301), Vβ8^{+}Vβ6^{+} (p=0.0103), Vβ14^{+}Vβ4^{+} (p=0.0456), and Vβ5^{+}Vβ4^{+} (p=0.0001) cells in *Ccnd3*$^{-/-}$*Atm*$^{-/-}$ mice (Fig. 5*A*,*B*). Relative to *WT* mice, we found 1.8 to 2.9 fold significantly higher frequencies of Vβ14^{+}Vβ6^{+} (p=0.008), Vβ5^{+}Vβ6^{+} (p=0.0035), Vβ14^{+}Vβ12^{+} (p=0.0298), Vβ5^{+}Vβ4^{+} (p=0.0001), and Vβ10^{+}Vβ4^{+} (p=0.0166) cells in *Ccnd3*$^{-/-}$ mice (Fig. 5*A*,*B*). These data demonstrate that Cyclin D3 cooperates with ATM to help enforce TCRβ allelic exclusion.

Discussion

Here, we have used flow cytometry to monitor allele-specific TCRβ or IgH expression and FISH to quantify bi-allelic VDJ rearrangements in wild-type and ATM-deficient mice. Our analyses of TCRβ and IgH expression and rearrangements in *Atm*$^{-/-}$ and wild-type mice demonstrate that ATM helps enforce TCRβ and IgH allelic exclusion by inhibiting the frequencies of mature T and B lymphocytes with bi-allelic VDJ rearrangements. While we detected elevated intracellular expression of TCRβ and IgH chains from both alleles in the pre-lymphocyte population of Atm-deficient mice as compared to Atm-deficient mice, we could not detect intracellular TCRβ or IgH allelic inclusion in pro-lymphocytes from either strain (Fig. S1, data not shown), likely due to the small numbers of pro-lymphocytes and the insensitivity of intracellular staining. Alternatively, the joining of persistent RAG DSBs during pro- to pre-lymphocyte differentiation could be a major means by which dual-Vβ/IgH expressing lymphocytes are generated. In this regard, such persistent RAG DSBs are observed at a low level in *WT* mice and at a higher level in *Atm*$^{-/-}$ mice (32,33). Asynchronous initiation of V-to-DJ recombination between alleles is required for TCRβ/IgH-mediated feedback inhibition to enforce allelic exclusion (6, 7). In the absence of any other means of V-to-DJ recombination control, the ability of feedback inhibition to enforce allelic exclusion would require efficient repair and expression of VDJ rearrangements on the first allele. Since ATM promotes coding join formation (29), the increased frequencies of *Atm*$^{-/-}$ cells with bi-allelic VDJ rearrangements could simply arise from inefficient repair of RAG DSBs on the first allele leading to V-to-DJ recombination on the second allele before activation of feedback inhibition signals. However, we previously used NHEJ-deficient pre-B cells to distinguish between ATM functions in DSB repair and signaling, thereby demonstrating that RAG DSBs induced on one allele during Igκ recombination signal through ATM to suppress Vκ-to-Jκ rearrangements on the other allele (8). Accordingly, the increased frequencies of *Atm*$^{-/-}$ lymphocytes with bi-allelic VDJ rearrangements could arise from loss of ATM signals that suppress additional V_H and Vβ rearrangements in response to RAG DSBs induced during V-to-DJ recombination on the first allele. We have not been able to assess contributions of these two non-mutually exclusive mechanisms using existing mouse models and *in vitro* systems of thymocyte and pro-B cell development. Thus, determining how ATM helps enforce TCRβ and IgH allelic exclusion by limiting bi-allelic VDJ rearrangements will require development of mouse models and/or systems of pro-lymphocyte development that distinguish between ATM functions in DSB repair versus signaling during the V-to-DJ recombination step.

Our analyses of TCRβ and IgH expression and rearrangements in *Ccnd3*$^{-/-}$ and wild-type mice show that Cyclin D3 helps enforce TCRβ and IgH allelic exclusion. V(D)J recombination is restricted to G1 phase cells by CyclinA/Cdk2-mediated phosphorylation and resultant degradation of RAG2 protein (34-36). In the 1990s, it was proposed that the ability of TCRβ chains to initiate signals that drive cells through G1 and into S phase, and thus inactivate RAG activity, is important to inhibit additional Vβ rearrangements and enforce TCRβ allelic exclusion (37,38). TCRβ and IgH expression in pro-T/B cells induces expression of Cyclin D3, which complexes with Cdk4 or Cdk6 kinases to drive cells through G1 and into S phase (11,12). We detected increased TCRβ and IgH allelic inclusion in *Ccnd3*$^{-/-}$ mice that correlated with an elevated frequency of bi-allelic $V_HD_HJ_H$ rearrangements. Although the latter was not significant from the numbers of cells analyzed, the ability to analyze orders of magnitude more cells by flow cytometry than by FISH renders detection of bi-allelic IgH expression more sensitive than bi-allelic V_H-to-D_HJ_H rearrangement. Consequently, our data is consistent with the notion that, after assembly of in-frame VDJ rearrangements on the first allele, *Ccnd3*$^{-/-}$ pro-lymphocytes have more time in G1 phase to initiate V rearrangements on the second allele. Since Cyclin D3 represses germline V_H transcription in pro-B cells (39), Cyclin D3 also could help enforce IgH allelic exclusion through down-regulation of V_H accessibility. Different domains of Cyclin D3 drive proliferation and inhibit V_H transcription (39). Thus, generation and analysis of mice expressing specific Cyclin D3 mutations will determine the contribution of each Cyclin D3 function to IgH and TCRβ allelic exclusion. Considering that neither CyclinD3/Cdk4 nor CyclinD3/Cdk6 complexes was tested for ability to control RAG2 protein stability (34, 35), Cyclin D3 also could regulate allelic exclusion through phosphorylation of RAG2 in G1 phase cells. We previously showed that Cyclin D3 inactivation had no effect on TCRβ-mediated feedback inhibition in mice expressing a pre-assembled functional TCRβ gene (40). Therefore, our current data that *Ccnd3*$^{-/-}$ mice exhibit increased TCRβ allelic inclusion provides further evidence that using pre-assembled functional genes/transgenes to study feedback inhibition and allelic exclusion has limitations (4,41,42).

Our analyses of TCRβ and IgH expression and rearrangements in *Atm*$^{-/-}$ and *Atm*$^{-/-}$*Ccnd3*$^{-/-}$ mice show that ATM and Cyclin D3 cooperate to help enforce TCRβ and IgH allelic exclusion. While the mechanisms that enforce TCRβ/IgH allelic exclusion have not yet been fully elucidated, it is well documented that TCRβ/IgH chains expressed from one allele signal permanent feedback inhibition of Vβ/V_H rearrangements on the other allele (3-5). Lymphocyte development-stage specific changes in TCRβ/IgH locus topology and accessibility likely prevent the re-initiation of Vβ/V_H rearrangement in pre-T/B cells (3-5), however evidence suggests that additional distinct mechanisms down-regulate Vβ/V_H recombination prior to TCRβ/IgH-signaled differentiation of pro-T/B cells (5). Our data indicates that activation of Cyclin D3 is one mechanism by which TCRβ/IgH-mediated signals suppress Vβ/V_H rearrangements in pro-T/B cells. For TCRβ/IgH-mediated feedback inhibition to enforce allelic exclusion, the field recognizes that additional mechanisms must promote asynchronous initiation of Vβ/VH rearrangements between alleles (3-5), although debate exists regarding the nature of these mechanisms due to inability to identify molecules that control this level of regulation (5). Our prior findings indicate that RAG cleavage during Vκ-to-Jκ recombination on one Igκ allele signals through ATM to transiently prevent RAG cleavage of the other Igκ allele (8). Our data here suggest a similar ATM-dependent mechanism helps enforce TCRβ/IgH allelic exclusion. Due to the many mechanisms that cooperate to enforce allelic exclusion, the absence of ATM and/or Cyclin D3 would be expected to result in much less than the theoretical maximum of TCRβ/IgH allelic inclusion (in 20% of lymphocytes and corresponding with bi-allelic V rearrangements in 100% of lymphocytes). In this context, our data showing bi-allelic V rearrangements in ~60% of ATM/Ccnd3-deficient cells, relative to ~40% of normal cells, indicates that asynchronous initiation and TCRβ/IgH-mediated feedback inhibition of V recombination cooperates with ATM-dependent and Ccnd3-dependent mechanisms to help enforce TCRβ/IgH allelic exclusion at normal levels. The theoretical maximum of TCRβ/IgH allelic inclusion also assumes that every TCRβ and IgH chain can functionally pair with every TCRα or IgL chain. Yet, the literature shows that this assumption is not valid (21,43). Moreover, the increased frequency of V(D)J coding end deletions that occur in ATM-deficient cells also would prevent achievement of the theoretical maximum level of TCRβ/IgH allelic inclusion in mice lacking ATM alone or both ATM and Cyclin D3. Although the effects of the loss of ATM and Cyclin D3 on TCRβ/IgH allelic exclusion are very small as expected, our data convincingly establishes that ATM and Cyclin D3 cooperate to help control mono-allelic Vβ/VH recombination.

Our data also demonstrate that inactivation of Cyclin D3 increases the frequency of $Atm^{-/-}$ B cells with bi-allelic IgH expression by suppressing aberrant V_H-to-D_HJ_H rearrangements that delete C_H genes. Impaired G1/S and G2/M checkpoints in $Atm^{-/-}$ cells enable RAG DSBs on non-selected alleles to persist un-repaired or become aberrantly repaired as cells proliferate (26,31,32). Accordingly, the simplest explanation for our data is that inactivation of Cyclin D3 provides $Atm^{-/-}$ pro-B cells with RAG DSBs on non-selected alleles more time in G1 to repair these lesions and assemble a second in-frame IgH gene. However, extended time in G1 phase and/or sustained germline V_H transcription after IgH expression in $Atm^{-/-}Ccnd3^{-/-}$ pro-B cells also could result in V_H rearrangements on non-selected alleles. Regardless, our data show that coordination of the V-to-DJ recombination step between alleles is important for suppressing aberrant rearrangements that cause deletion or translocation of TCRβ or IgH genes on non-selected alleles. Although such genomic lesions cannot cause bi-allelic expression of TCRβ or IgH loci, they could inactivate tumor suppressor genes or activate oncogenes.

Inherited ATM deficiency in humans causes Ataxia Telangiectasia (A-T), a disorder associated with lymphopenia, immunodeficiency, elevated frequency of Ig and TCR translocations in lymphocytes, increased predisposition to lymphoid cancers with oncogenic Ig or TCR translocations, and elevated risk of autoimmune disease (44-46). The increased frequencies of Ig and TCR translocations and resultant lymphoid cancers of A-T patients is thought to arise from impaired DSB repair and cell cycle checkpoints in their lymphocytes (29). Our data suggest that inability of A-T cells to properly coordinate initiation of RAG DSBs between alleles during TCRβ and IgH recombination may contribute to these phenotypes. The higher risk of autoimmunity in A-T patients is thought to develop as a result of their lymphopenia caused by impaired development, proliferation, and survival of lymphocytes (42,47,48). Antigen receptor allelic exclusion is widely hypothesized to suppress autoimmunity by ensuring negative selection of lymphocytes that express autoreactive antigen receptors (4,5). In support of this idea, studies with mice expressing TCRβ or IgH transgenes or an Igκ allotypic marker have shown that lack of allelic exclusion permits autoreactive cells to escape deletion and/or accumulate in the periphery (22, 49-51). Thus, our data also suggest that the increased risk of autoimmunity in A-T patients could develop, at least in part, from impaired enforcement of antigen receptor allelic exclusion. Since discovery of IgH allelic exclusion in 1965 (52), the relevance of allelic exclusion for human health has remained an enigma due to lack of natural or engineered mutations that increase the frequencies of lymphocytes with bi-allelic expression of diverse antigen receptor gene repertoires. Our finding that ATM and Cyclin D3 cooperate to help enforce TCRβ or IgH allelic exclusion finally provides experimental means to investigate the consequence of increasing bi-allelic expression of these antigen receptor genes.

Supplementary Material

Refer to Web version on PubMed Central for supplementary material.

Acknowledgments

[2]This research was supported by a Cancer Research Institute Pre-doctoral Emphasis Pathway in Tumor Immunology Training Grant (N.C.S.), a Leukemia and Lymphoma Scholar Award (C.H.B.) and the National Institutes of Health Grants R01 CA125195 (C.H.B.) and R01 CA136470 (C.H.B.).

References

1. Schatz DG, Swanson PC. V(D)J recombination: mechanisms of initiation. Ann. Rev. Gen. 2011; 45:167–202.
2. Helmink BA, Sleckman BP. The response to and repair of RAG-mediated DNA double-strand breaks. Annu. Rev. Immunol. 2012; 30:175–202. [PubMed: 22224778]
3. Mostoslavasky R, Alt FW, Rajewsky K. The lingering enigman of the allelic exclusion mechanism. Cell. 2004; 3:539–544.
4. Brady BL, Steinel NC, Bassing CH. Antigen receptor allelic exclusion: an update and reappraisal. J. Immunol. 2010; 185:3801–3808. [PubMed: 20858891]
5. Vettermann C, Schlissel MS. Allelic exclusion of immunoglobulin genes: models and mechanisms. Immunol. Rev. 2010; 237:22–42. [PubMed: 20727027]
6. Alt FW, Enea V, Bothwell AL, Baltimore D. Activity of multiple light chain genes in murine myeloma cells producing a single, functional light chain. Cell. 1980; 21:1–12. [PubMed: 6773666]
7. Hewitt SL, Yin B, Ji Y, Chaumeil J, Marszalek K, Tenthorey J, Salvagiotto G, Steinel N, Ramsey LB, Ghysdael J, Farrar MA, Sleckman BP, Schatz DG, Busslinger M, Bassing CH, Skok JA. RAG-1 and ATM coordinate monoallelic recombination and nuclear positioning of immunoglobulin loci. Nat. Immunol. 2009; 10:655–664. [PubMed: 19448632]
8. Steinel NC, Lee BS, Tubbs AT, Bednarski JJ, Schulte E, Yang-Iott KS, Schatz DG, Sleckman BP, Bassing CH. The ataxia telangiectasia mutated kinase controls Igkappa allelic exclusion by inhibiting secondary Vkappa-to-Jkappa rearrangements. J. Exp. Med. 2013; 210:233–239. [PubMed: 23382544]
9. Jackson AM, Krangel MS. Turning T-cell receptor beta recombination on and off: more questions than answers. Immunol. Rev. 2006; 209:129–141. [PubMed: 16448539]
10. Jung D, Giallourakis C, Mostoslavsky R, Alt FW. Mechanism and control of V(D)J recombination at the immunoglobulin heavy chain locus. Annu. Rev. Immunol. 2006; 24:541–570. [PubMed: 16551259]
11. Sicinska E, Aifantis I, Le Cam L, Swat W, Borowski C, Yu Q, Ferrando AA, Levin SD, Geng Y, von Boehmer H, Sicinski P. Requirement for cyclin D3 in lymphocyte development and T cell leukemias. Cancer Cell. 2003; 4:451–461. [PubMed: 14706337]
12. Cooper AB, Sawai CM, Sicinska E, Powers SE, Sicinski P, Clark MR, Aifantis I. A unique function for cyclin D3 in early B cell development. Nat. Immunol. 2006; 7:489–497. [PubMed: 16582912]
13. Kreslavsky T, Gleimer M, Miyazaki M, Choi Y, Gagnon E, Murre C, Sicinski P, von Boehmer H. β-selection-induced proliferation is required for αβ T cell differentiation. Immunity. 2012; 37:840–853. [PubMed: 23159226]
14. Aifantis I, Buer J, von Boehmer H, Azogui O. Essential role of the pre-T cell receptor in allelic exclusion of the T cell receptor beta locus. Immunity. 1997; 7:601–607. [PubMed: 9390684]
15. Balomenos D, Balderas RS, Mulvany KP, Kaye J, Kono DH, Theofilopoulos AN. Incomplete T cell receptor V beta allelic exclusion and dual V beta-expressing cells. J. Immunol. 1995; 155:3308–3312. [PubMed: 7561023]
16. Barreto V, Cumano A. Frequency and characterization of phenotypic Ig heavy chain allelically included IgM-expressing B cells in mice. J. Immunol. 2000; 164:893–899. [PubMed: 10623837]
17. ten Boekel E, Melchers F, Rolink AG. Precursor B cells showing H chain allelic inclusion display allelic exclusion at the level of pre-B cell receptor surface expression. Immunity. 1998; 8:199–207. [PubMed: 9492001]

18. Mostoslavasky R, Singh N, Kirillov A, Pelanda R, Cedar H, Chess A, Bergman Y. Kappa chain monoallelic demethylation and the establishment of allelic exclusion. Genes Dev. 1998; 12:1801–1811. [PubMed: 9637682]
19. Nemazee D. Receptor editing in lymphocyte development and central tolerance. Nat. Rev. Immunol. 2006; 6:728–740. [PubMed: 16998507]
20. Pelenda R, Torres RM. Receptor editing for better or for worse. Curr. Opin. Immunol. 2006; 18:184–190. [PubMed: 16460922]
21. Casellas R, Zhang Q, Zheng NY, Mathias MD, Smith K, Wilson PC. Igkappa allelic inclusion is a consequence of receptor editing. J. Exp. Med. 2007; 204:153–160. [PubMed: 17210730]
22. Fournier EM, Velez MG, Leahy K, Swanson CL, Rubtsov AV, Torres RM, Pelenda R. Dual-reactive B cells are autoreactive and highly enriched in the plasmablast and memory B cell subsets of autoimmune mice. J. Exp. Med. 2012; 209:1797–1812. [PubMed: 22927551]
23. Wu C, Bassing CH, Jung D, Woodman BB, Foy D, Alt FW. Dramatically increased rearrangement and peripheral representation of Vbeta14 driven by the 3'Dbeta1 recombination signal sequence. Immunity. 2003; 18:75–85. [PubMed: 12530977]
24. Carpenter AC, Yang-Iott KS, Chao LH, Nuskey B, Whitlow S, Alt FW, Bassing CH. Assembled DJ beta complexes influence TCR beta chain selection and peripheral V beta repertoire. J. Immunol. 2009; 182:5586–5595. [PubMed: 19380806]
25. Steinel NC, Brady BL, Carpenter AC, Yang-Iott KS, Bassing CH. Posttranscriptional silencing of VbetaDJbetaCbeta genes contributes to TCRbeta allelic exclusion in mammalian lymphocytes. J. Immunol. 2010; 185:1055–1062. [PubMed: 20562258]
26. Mahowald GK, Baron JM, Mahowald MA, Kulkarni S, Bredemeyer AL, Bassing CH, Sleckman BP. Aberrantly resolved RAG-mediated DNA breaks in Atm-deficient lymphocytes target chromosomal breakpoints in cis. Proc. Natl. Acad. Sci. USA. 2009; 106:18339–18344. [PubMed: 19820166]
27. Ranganath S, Carpenter AC, Gleason M, Shaw AC, Bassing CH, Alt FW. Productive coupling of accessible Vbeta14 segments and DJbeta complexes determines the frequency of Vbeta14 rearrangement. J. Immunol. 2008; 180:2339–2346. [PubMed: 18250443]
28. Alt FW, Yancopoulos GD, Blackwell TK, Wood C, Thomas E, Boss M, Coffman R, Rosenberg N, Tonegawa S, Baltimore D. Ordered rearrangement of immunoglobulin heavy chain variable region segments. EMBO J. 1984; 3:1209–1219. [PubMed: 6086308]
29. Bredemeyer AL, Sharma GG, Huang CY, Helmink BA, Walker LM, Khor KC, Nuskey B, Sullivan KE, Pandita TK, Bassing CH, Sleckman BP. ATM stabilizes DNA double-strand-break complexes during V(D)J recombination. Nature. 2006; 442:466–470. [PubMed: 16799570]
30. Kaushik A, Schulze DH, Bonilla FA, Bona C, Kelsoe G. Stochastic pairing of heavy-chain and kappa light-chain variable gene families occurs in polyclonally activated B cells. Proc. Natl. Acad. Sci. USA. 1990; 87:4932–4936. [PubMed: 2114644]
31. Callen E, Jankovic M, Difilippantonio S, Daniel JA, Chen HT, Celeste A, Pellegrini M, McBride K, Wangsa D, Bredemeyer AL, Sleckman BP, Ried T, Nussenzweig M, Nussenzweig A. ATM prevents the persistence and propagation of chromosome breaks in lymphocytes. Cell. 2007; 130:63–75. [PubMed: 17599403]
32. Dujka ME, Puebla-Osorio N, Tavana O, Sang M, Zhu C. ATM and p53 are essential in the cell-cycle containment of DNA breaks during V(D)J recombination in vivo. Oncogene. 2010; 29:957–965. [PubMed: 19915617]
33. Pedraza-Alva G, Koulnis M, Charland C, Thornton T, Clements JL, Schlissel MS, Rincon M. Activation of p38 MAP kinase by DNA double-strand breaks in V(D)J recombination induces a G2/M cell cycle checkpoint. EMBO J. 2006; 25:763–773. [PubMed: 16456545]
34. Lin W-C, Desiderio S. Regulation of V(D)J recombination activator protein RAG-2 by phosphorylation. Science. 1993; 260:953–959. [PubMed: 8493533]
35. Lee J, Desiderio S. Cyclin A/CDK2 regulates V(D)J recombination by coordinating RAG-2 accumulation and DNA repair. Immunity. 1999; 11:771–781. [PubMed: 10626899]
36. Jiang H, Chang FC, Ross AE, Lee J, Nakayama K, Nakayama K, Desiderio S. Ubiquitylation of RAG-2 by Skp2-SCF links destruction of the V(D)J recombinase to the cell cycle. Molec. Cell. 2005; 18:699–709. [PubMed: 15949444]

37. Dudley EC, Petrie HT, Shah LM, Owen MJ, Hayday AC. T cell receptor beta chain gene rearrangement and selection during thymocyte development in adult mice. Immunity. 1994; 1:83–93. [PubMed: 7534200]
38. Hoffman ES, Passoni L, Crompton T, Leu TM, Schatz DG, Koff A, Owen MJ, Hayday AC. Productive T-cell receptor beta-chain gene rearrangement: coincident regulation of cell cycle and clonality during development in vivo. Genes Dev. 1996; 10:948–962. [PubMed: 8608942]
39. Powers SE, Mandal M, Matsuda S, Miletic AV, Cato MH, Tanaka A, Rickert RC, Koyasu S, Clark MR. Subnuclear cyclin D3 compartments and the coordinated regulation of proliferation and immunoglobulin variable gene repression. J. Exp. Med. 2012; 209:2199–2213. [PubMed: 23109711]
40. Brady BL, Bassing CH. Differential regulation of proximal and distal Vbeta segments upstream of a functional VDJbeta1 rearrangement upon beta-selection. J. Immunol. 2011; 187:3277–3285. [PubMed: 21844384]
41. Brady BL, Oropallo MA, Yang-Iott KS, Serwold T, Hochedlinger K, Jaenisch R, Weissman IL, Bassing CH. Position-dependent silencing of germline Vb segments on TCRb alleles containing preassembled VbDJbCb1 genes. J. Immunol. 2010; 185:3564–3573. [PubMed: 20709953]
42. Gartner F, Alt FW, Monroe R, Chu M, Sleckman BP, Davidson L, Swat W. Immature thymocytes employ distinct signaling pathways for allelic exclusion versus differentiation and expansion. Immunity. 1999; 10:537–546. [PubMed: 10367899]
43. Casanova JL, Romero P, Wildman C, Kourilsky P, Maryanski JL. T cell receptor genes in a series of class I major histocompatibility complex-restricted cytotoxic T lymphocyte clones specific for a *Plasmodium berghei* nonapeptide: implications for T cell allelic exclusion and antigen-specific repertoire. J. Exp. Med. 1991; 174:1371–1383. [PubMed: 1836010]
44. Ammann AJ, Hong R. Autoimmune phenomena in ataxia telangiectasia. J. Pediatr. 1971; 78:821–826. [PubMed: 4932023]
45. Patiroglu T, Gungor HE, Unal E. Autoimmune diseases detected in children with primary immunodeficiency diseases: results form a reference centre at middle anatolia. Acta Microbiol. Immunol. Hung. 2012; 59:343–353. [PubMed: 22982638]
46. Ambrose M, Gatti RA. Pathogenesis of ataxia-telangiectasia: the next generation of ATM functions. Blood. 2013; 121:4036–4045. [PubMed: 23440242]
47. Kaufman DB, Miller HC. Ataxia telangiectasia: an autoimmune disease associated with a cytotoxic antibody to brain and thymus. Clin. Immunol. Immunopathol. 1977; 7:288–299. [PubMed: 324682]
48. Shao L, Fujii H, Colmegna I, Oishi H, Goronzy JJ, Weyand CM. Deficiency of the DNA repair enzyme ATM in rheumatoid arthritis. J. Exp. Med. 2009; 206:1435–1449. [PubMed: 19451263]
49. Iliev A, Spatz L, Ray S, Diamond B. Lack of allelic exclusion permits autoreactive B cells to scape deletion. J. Immunol. 1994; 153:3551–3556. [PubMed: 7930577]
50. Zal T, Weiss S, Mellor A, Stockinger B. Expression of a second receptor rescues self-specific T cells from thymic deletion and allows activation of autoreactive effector function. Proc. Natl. Acad. Sci. USA. 1996; 93:9102–9107. [PubMed: 8799161]
51. Sarukhan A, Garcia C, Lanoue A, von Boehmer H. Allelic inclusion of T cell receptor alpha genes poses an autoimmune hazard due to low-level expression of autospecific receptors. Immunity. 1998; 8:563–570. [PubMed: 9620677]
52. Pernis B, Chiappino G, Kelus AS, Gell PG. Cellular localization of immunoglobulins with different allotypic specificities in rabbit lymphoid tissues. J. Exp. Med. 1965; 122:853–876. [PubMed: 4159057]

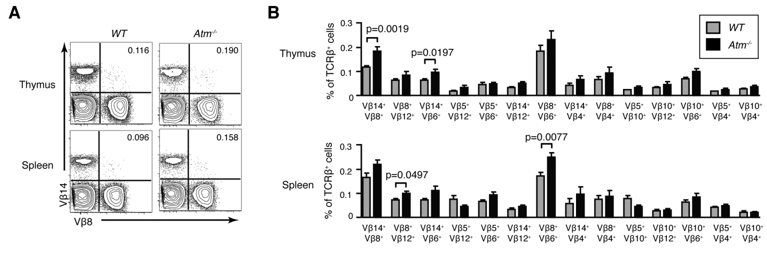

	#	VDJ/DJ	VDJ/VDJ	VDJ/Ab
Fusion 1	85	41	34	11
Fusion 2	38	7	17	14
Fusion 3	67	22	25	20
Total	190	70	76	44

FIGURE 1.

ATM helps control TCRβ allelic exclusion and TCRβ recombination. *A*, Representative flow cytometry analysis of Vβ14 and Vβ8 expression on the surface of TCRβ^{+} thymocytes or splenocytes isolated from *WT* or *Atm*$^{-/-}$ mice. The percentages of Vβ14^{+}Vβ8^{+} αβ T cells in the upper right quadrant are shown. *B*, Graphs depicting the average frequencies of TCRβ^{+}B220^{-} thymocytes or splenocytes isolated from *WT* or *Atm*$^{-/-}$ mice that express each indicated combination of surface Vβ chains. Data are from four independent experiments conducted on a total of eight *WT* and ten *Atm*$^{-/-}$ littermate mice. Error bars indicate the SEM. *C*, Diagram of the TCRβ locus illustrating the relative positions of the upstream Vβ segments, the two Dβ-Jβ-Cβ clusters, and the downstream Vβ14 segment. Locations of the *EcoR*I sites and 5'Dβ1, 3'Jβ1, and 3'Jβ2 probes used for Southern blot analysis of TCRβ rearrangements are indicated. *D*, Table depicting the frequencies of *Atm*$^{-/-}$ αβ T cell hybridomas with a normal VβDβJβ rearrangement on one (VDJ/DJ) or both (VDJ/VDJ) alleles, or with a normal VβDβJβ rearrangement on one allele and an aberrant *Tcrb* rearrangement on the other allele (VDJ/Ab).

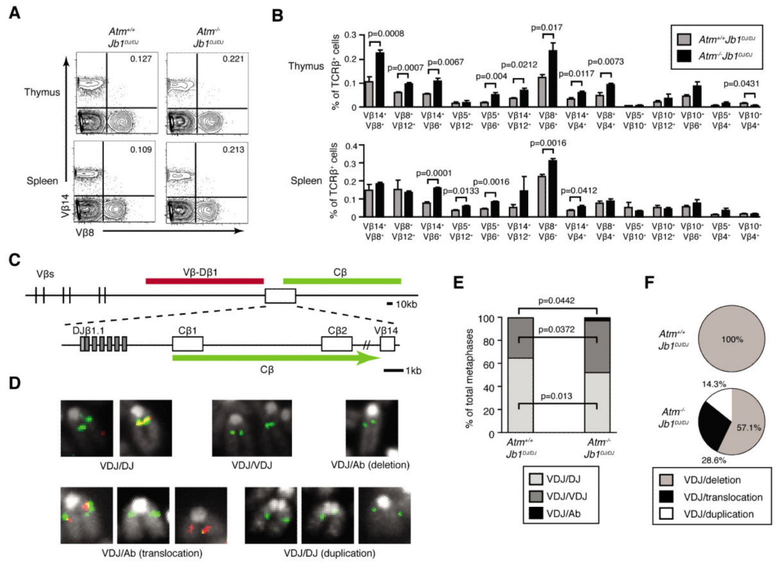

FIGURE 2.

ATM enforces TCRβ allelic exclusion, inhibits bi-allelic Vβ-to-DβJβ recombination, and suppresses aberrant Vβ rearrangements. *A*, Representative flow cytometry analysis of Vβ14 and Vβ8 expression on the surface of TCRβ$^+$B220$^-$ thymocytes or splenocytes isolated from *Atm*$^{+/+}$*Jb1*$^{DJ/DJ}$ or *Atm*$^{-/-}$*Jb1*$^{DJ/DJ}$ mice. The percentages of Vβ14$^+$Vβ8$^+$ αβ T cells are shown in the upper right quadrant. *B*, Graphs depicting the average frequencies of TCRβ$^+$B220$^-$ thymocytes or splenocytes isolated from *Atm*$^{+/+}$*Jb1*$^{DJ/DJ}$ or *Atm*$^{-/-}$*Jb1*$^{DJ/DJ}$ mice that express each indicated combination of surface Vβ chains. Data are from two independent experiments conducted on a total of six *Atm*$^{+/+}$*Jb1*$^{DJ/DJ}$ and six *Atm*$^{-/-}$*Jb1*$^{DJ/DJ}$ littermate mice. Error bars indicate the SEM. *C*, Diagram of the *Jb1*^{DJ} locus illustrating the relative positions of upstream Vβ segments, the two Dβ-Jβ-Cβ clusters, and the downstream Vβ14 segment. Locations of the Vβ-Dβ1 and Cβ probes used for 2C-FISH analysis of Vβ rearrangements are indicated. *D*, Representative 2C-FISH images showing the metaphase chromosome probe hybridization patterns that identify *Atm*$^{+/+}$*Jb1*$^{DJ/DJ}$ or *Atm*$^{-/-}$*Jb1*$^{DJ/DJ}$ αβ T cells with a normal VβDβJβ rearrangement on one (VDJ/DJ) or both (VDJ/VDJ) alleles, or with a normal VβDβJβ rearrangement on one allele and an aberrant TCRβ rearrangement on the other allele (VDJ/Ab). *E-F*, Graphs depicting the average frequencies of *Atm*$^{+/+}$*Jb1*$^{DJ/DJ}$ and *Atm*$^{-/-}$*Jb1*$^{DJ/DJ}$ splenic αβ T cells with TCRβ alleles of the VDJ/DJ, VDJ/VDJ, or VDJ/Ab configurations (*E*), or the frequencies of the types aberrant TCRβ rearrangements in *Atm*$^{+/+}$*Jb1*$^{DJ/DJ}$ and *Atm*$^{-/-}$*Jb1*$^{DJ/DJ}$ splenic αβ T cells (*F*). Data are from 388 *Atm*$^{+/+}$*Jb1*$^{DJ/DJ}$ and 234 *Atm*$^{-/-}$*Jb1*$^{DJ/DJ}$ metaphase analyzed among four independent experiments.

NIH-PA Author Manuscript
NIH-PA Author Manuscript

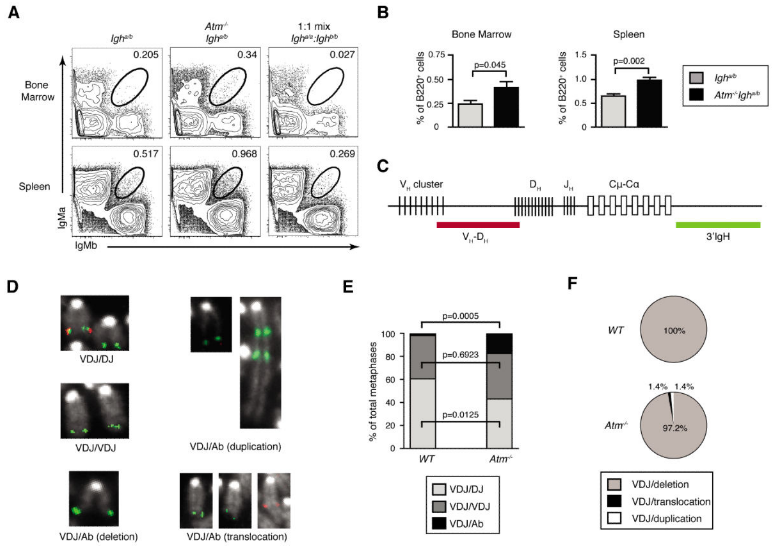

FIGURE 3.

ATM helps enforce IgH allelic exclusion, inhibit bi-allelic V_H-to-D_HJ_H recombination, and suppress aberrant V_H rearrangements. *A*, Representative flow cytometry analysis of IgM^a and IgM^b expression on the surface of $B220^+TCR\beta^-$ bone marrow cells or splenocytes isolated from *Atm*$^{+/+}$*Igh*$^{a/b}$ or *Atm*$^{-/-}$*Igh*$^{a/b}$ mice. The circle gates capture B cells expressing equivalent high levels of both IgM^a and IgM^b on their surface. The percentages of cells in these gates are indicated. The position of these gates was determined from a 1:1 mix of *Igh*$^{a/a}$ and *Igh*$^{b/b}$ stained cells as shown. *B*, Graphs depicting the average frequencies of B cells in the bone marrow or spleens of *Atm*$^{+/+}$*Igh*$^{a/b}$ or *Atm*$^{-/-}$*Igh*$^{a/b}$ mice that express both IgM^a and IgM^b on their surface. Data are from three independent experiments conducted on a total of six *Atm*$^{+/+}$*Igh*$^{a/b}$ and seven *Atm*$^{-/-}$*Igh*$^{a/b}$ littermate mice. Error bars indicate SEM. *C*, Diagram of the IgH locus illustrating the relative positions of V_H, D_H, and J_H segments and the downstream C_H exons for each Ig class. Locations of the V_H-D_HJ_H and 3'IgH probes used for 2C-FISH analysis of IgH rearrangements are shown. *D*, Representative 2C-FISH images showing metaphase chromosome probe hybridization patterns that identify *Atm*$^{+/+}$ or *Atm*$^{-/-}$ B cells with a normal $V_HD_HJ_H$ rearrangement on one (VDJ/DJ) or both (VDJ/VDJ) alleles, or with a normal $V_HD_HJ_H$ rearrangement on one allele and an aberrant $V_HD_HJ_H$ rearrangement on the other allele (VDJ/Ab). *E*-*F*, Graphs depicting the average frequencies of *Atm*$^{+/+}$ and *Atm*$^{-/-}$ splenic B cells with *Igh* alleles of the VDJ/DJ, VDJ/VDJ, or VDJ/Ab configurations (*E*), or the frequencies of the indicated types aberrant IgH rearrangements in *Atm*$^{+/+}$ and *Atm*$^{-/-}$ splenic B cells (*F*). Data are from 410 *Atm*$^{+/+}$ and 410 *Atm*$^{-/-}$ metaphases analyzed among four independent experiments.

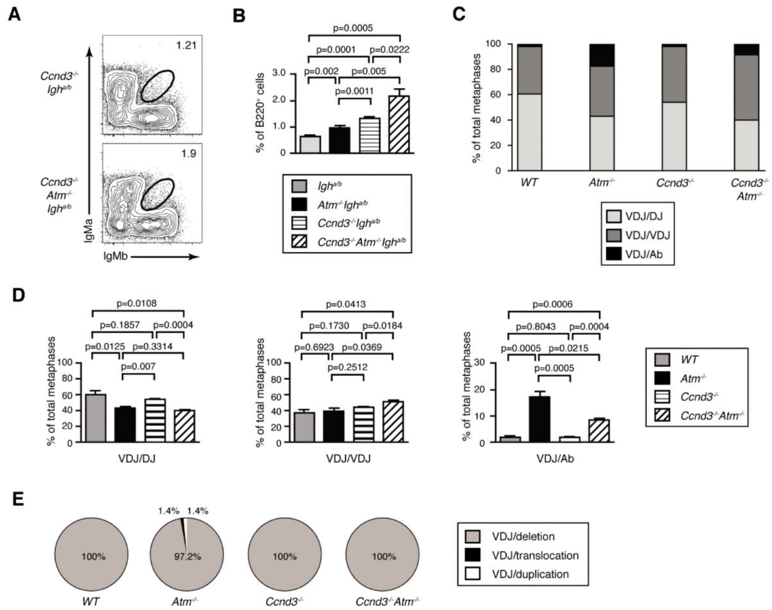

FIGURE 4.

ATM and Cyclin D3 cooperate to help enforce IgH allelic exclusion, inhibit bi-allelic V_H-to-D_HJ_H recombination, and suppress aberrant V_H rearrangements. *A*, Representative flow cytometry analysis of IgM^a and IgM^b expression on $B220^+TCR\beta^-$ splenocytes isolated from *Ccnd3*$^{-/-}$*Igh*$^{a/b}$ or *Ccnd3*$^{-/-}$*Atm*$^{-/-}$*Igh*$^{a/b}$ mice. The circle gates capture splenic B cells expressing equivalent high levels of both IgM^a and IgM^b on their surface. The percentages of cells in these gates are indicated. *B*, Graphs depicting the average frequencies of B cells in the spleens of *Atm*$^{+/+}$*Igh*$^{a/b}$, *Atm*$^{-/-}$*Igh*$^{a/b}$, *Ccnd3*$^{-/-}$*Igh*$^{a/b}$, or *Ccnd3*$^{-/-}$*Atm*$^{-/-}$*Igh*$^{a/b}$ mice that express both IgM^a and IgM^b on their surface. The data for *Atm*$^{+/+}$*Igh*$^{a/b}$ and *Atm*$^{-/-}$*Igh*$^{a/b}$ mice is the same from Figure 3. Data are from three independent experiments conducted on a total of six *Atm*$^{+/+}$*Igh*$^{a/b}$ and eight *Atm*$^{-/-}$*Igh*$^{a/b}$ littermate mice. Error bars indicate SEM. *C-E*, Graphs depicting the average frequencies of *Atm*$^{+/+}$, *Atm*$^{-/-}$, *Ccnd3*$^{-/-}$, or *Ccnd3*$^{-/-}$*Atm*$^{-/-}$ splenic B cells with IgH alleles of the VDJ/DJ, VDJ/VDJ, or VDJ/Ab configurations (*C-D*), or the frequencies of the types of aberrant IgH rearrangements in *Ccnd3*$^{-/-}$ or *Ccnd3*$^{-/-}$*Atm*$^{-/-}$ splenic B cells (*E*). Data for *Atm*$^{+/+}$*Igh*$^{a/b}$ and *Atm*$^{-/-}$*Igh*$^{a/b}$ mice are from Figure 3. Data are from 404 *Ccnd3*$^{-/-}$ and 309 *Ccnd3*$^{-/-}$*Atm*$^{-/-}$ metaphases analyzed among three independent experiments. Error bars indicate SEM. Error bars are not displayed in C, but are in D, since the same data is shown in both C and D.

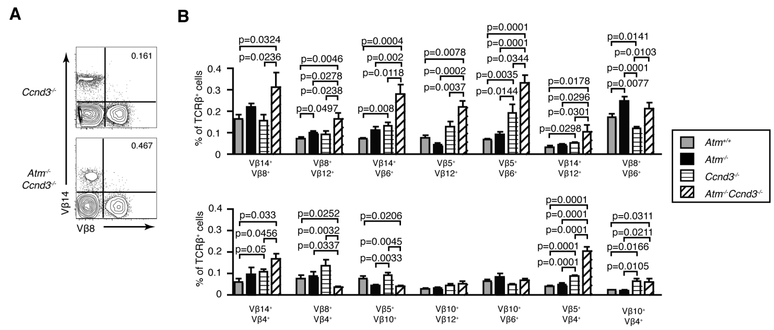

FIGURE 5.

ATM and Cyclin D3 cooperate to enforce TCRβ allelic exclusion. *A*, Representative flow cytometry analysis of Vβ14 and Vβ8 expression on the surface of splenic αβ T cells isolated from *Ccnd3*$^{-/-}$ or *Ccnd3*$^{-/-}$*Atm*$^{-/-}$ mice. The percentages of Vβ14^{+}Vβ8^{+} αβ T cells in the upper right quadrant are shown. *B*, Graphs depicting the average frequencies of splenic αβ T cells from *Atm*$^{+/+}$, *Atm*$^{-/-}$, *Ccnd3*$^{-/-}$, or *Ccnd3*$^{-/-}$*Atm*$^{-/-}$ mice that express each indicated combination of surface Vβ chains. The data for *Atm*$^{+/+}$ and *Atm*$^{-/-}$ mice are from Figure 3. Data are from three independent experiments conducted on a total of eight *Ccnd3*$^{-/-}$ and six *Ccnd3*$^{-/-}$*Atm*$^{-/-}$ littermate mice. Error bars indicate SEM.